THE ASTROPHYSICAL JOURNAL, 371:525–534, 1991 April 20

OX 169: EVIDENCE FOR A RECENT MERGER

ALAN STOCKTON[1,2] AND TONY FARNHAM[1]
Institute for Astronomy, 2680 Woodlawn Drive, University of Hawaii, Honolulu, HI 96822
Received 1990 August 11; accepted 1990 October 2

ABSTRACT

We present new imaging and spectroscopy of the faint jetlike structure extending to the southeast from the luminous QSO OX 169 as well as new observations of the unusual double-peaked broad Balmer lines in the spectrum of the QSO itself. The luminosity of the "jet" is clearly of stellar origin, and the feature is apparently a planar distribution of stars seen edge-on. However, because of its strong asymmetry, it cannot be a normal galactic disk and, by analogy with other objects seen roughly face-on, is quite plausibly a tidal tail.

Previous discussions of the double-peaked Balmer lines in OX 169 have suggested Balmer self-absorption in an intervening broad-line cloud or a superposition of broad- and narrow-line profiles at different redshifts. More recently, double-peaked broad lines in other objects have been interpreted in terms of Keplerian disk models. We see significant differences in the Hβ profile between spectra of OX 169 obtained in 1983 and 1989: while a relativistic disk model is an excellent fit to the 1989 profile, no such profile can fit the 1983 profile unless azimuthal asymmetries are introduced. These differential variations in two spectra obtained 6 yr apart allow us to perform a rough deconvolution of the profile and to show that the broad-line radiation likely arises in two essentially independent regions. A bipolar geometry remains a possibility, but a supermassive binary, each component with its own broad-line region, is attractive because such a model can encompass additional phenomena often observed in active nuclei. If this latter explanation is, in fact, correct, then the two observationally disparate phenomena we discuss in this paper could have a common physical origin.

Subject headings: galaxies: individual (OX 169) — galaxies: jets — galaxies: structure — quasars — radio sources: galaxies

1. INTRODUCTION

This paper deals with two unusual features associated with the QSO OX 169: one morphological, the other spectroscopic. The former is the jetlike projection extending about 10″ from OX 169 at position angle 120° (Stockton 1978; Hutchings et al. 1984b; Gehren et al. 1984; Smith et al. 1986; Heckman et al. 1986); the latter is the double-peaked appearance of the broad emission-line profiles in the spectrum of the QSO itself (Smith 1980). We hope to show that both of these phenomena, though apparently rare among active galaxies, are nevertheless of general interest. It is even possible that the two are related.

OX 169 is a fairly luminous QSO with a redshift of 0.21. It is also an unresolved flat-spectrum radio source (Feigelson, Isobe, & Kembhavi 1984; Gower & Hutchings 1984) and a rapid X-ray variable (Zamorani et al. 1984). Weak, patchy extended emission is present to the south of the QSO (Stockton & MacKenty 1987). We present here new imaging observations in the optical, infrared, and radio, as well as the results of spectroscopy of both the nucleus and the jet. The observational material on which this paper is based is summarized in Table 1. Our observations of the jet and interpretation of its nature are given in § 2, and the observations of the broad emission lines and a discussion of possible models for the broad-line region are given in § 3. In § 4, we attempt to evaluate implications of our results for an integrated understanding of OX 169 as well as in the larger context of active galaxies generally.

[1] Visiting Astronomer, Canada-France-Hawaii Telescope, operated by the National Research Council of Canada, the Centre National de la Recherche Scientifique of France, and the University of Hawaii.

[2] Visiting Astronomer, United Kingdom Infrared Telescope, operated by the Royal Observatory Edinburgh on behalf of the United Kingdom Science and Engineering Research Council and the Netherlands Organization for Scientific Research.

2. THE JETLIKE FEATURE

1.1. *Introduction*

A deep image of OX 169 is shown as Figure 1 (Plate 21). For brevity, we will refer to the projection to the south-east as the "jet," without intending any prejudgment of its physical properties. There is also a stubby collinear counterpart to this feature on the opposite side of the QSO, but it is clear from this image and from other deep images, such as those shown by Heckman et al. (1986) and Stockton & MacKenty (1987), that the striking asymmetry between the two sides persists in images having limiting surface brightnesses well below the mean surface brightness of the jet, and is, in fact, a fundamental aspect of the morphology of the system. A contour plot of the latter image is shown here as Figure 2. As a number of investigations (Gehren et al. 1984; Hutchings, Crampton, & Campbell 1984; Smith et al. 1986) have made clear, the host galaxy of OX 169 is quite luminous, and the lower contours of Figure 2 clearly show the spheroidal distribution of material centered on the QSO nucleus.

2.2. *Imaging and Spectroscopic Observations*

We obtained images of OX 169 at the Cassegrain focus of the Canada-France-Hawaii Telescope (CFHT) with a focal reducer giving a final scale of 0.″3 pixel^{-1} on the Galileo/IfA TI 500 × 500 CCD. Six 60 s integrations were taken through each of two filters. The first was an interference filter that is similar in central wavelength and bandwidth to the Thuan & Gunn (1976) g band; the second, an RG 665 filter with a cutoff at 7060 Å. The raw images were reduced in a standard manner,

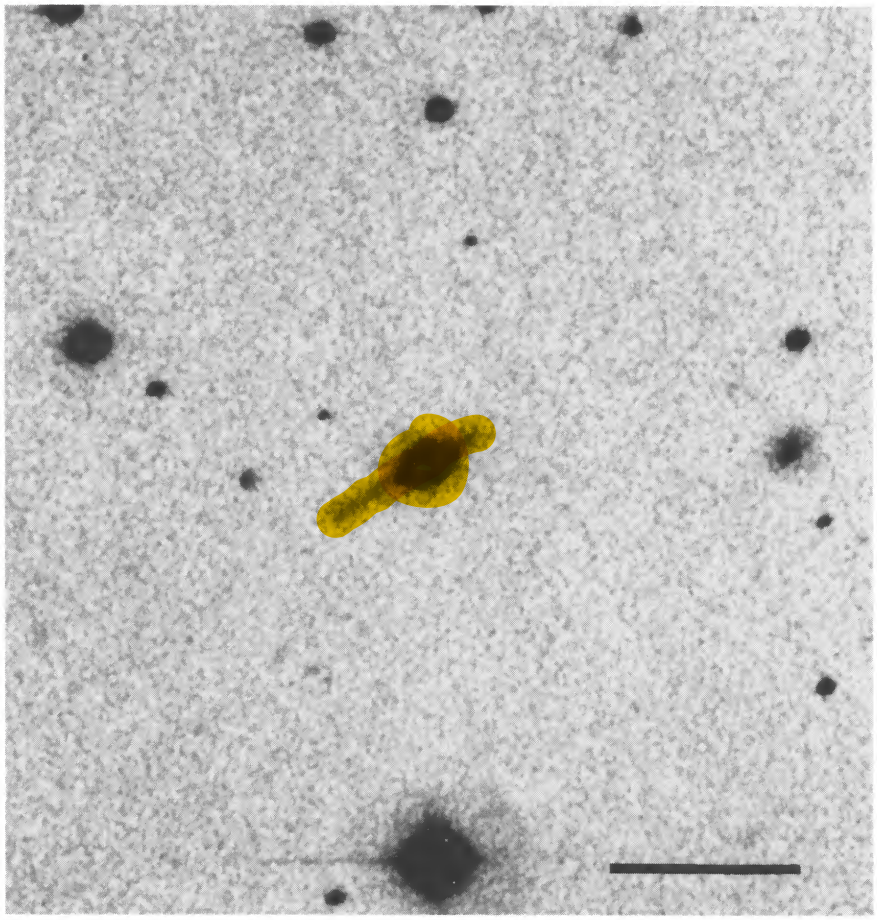

FIG. 1.—Image of OX 169 obtained at the CFHT Cassegrain focus with the Galileo/IfA CCD a focal reducer giving a scale of 0.3 arcsec pixel^{-1}. The image is a median average of six 60 s exposures through an RG-665 filter with an interference cutoff at 7200 Å. North is up, east to the left, and the scale bar on the illustration is 20″ long.

TABLE 1

JOURNAL OF OBSERVATIONS

Date	Telescope	Exposure	Remarks
1982 Mar 8	VLA	3 × 600 s	A-array, 6 cm
1983 Sep 8	UH 2.2 m	9000 s	TI 500 × 500 CCD
1984 May 26	UH 2.2 m	9 × 450 s	Bandpass 5730–6230 Å; TI 500 × 500 CCD
1985 Oct 16	CFHT	6 × 60 s (g′)	Bandpass 4550–5500 Å
		6 × 60 s (R′)	Bandpass 6680–7060 Å; TI 500 × 500 CCD
1986 Jul 6	CFHT	2 × 5100 s	Spectrum; 5097–6415 Å; 20 Å resolution; TI 500 × 500 CCD
1988 Oct 5	UKIRT	36 × 60 s	*K* band; IRCAM (58 × 62)
1989 Sep 1, 2	UH 2.2 m	3 × 3600 s, 2 × 4800 s	Spectrum; 4509–5484 Å; 20 Å resolution; TI 800 × 800 CCD
1989 Sep 1	UH 2.2 m	3600 s	Hα, 10 Å resolution; TI 800 × 800 CCD
1989 Sep 2, 3	UH 2.2 m	3000 s, 2 × 3600 s	Hβ, 5 Å resolution; TI 800 × 800 CCD
1989 Sep 3	UH 2.2 m	4200s	Hγ, 5 Å resolution; TI 800 × 800 CCD

the flat-field frame being generated from the medianed sky background of the image frames.

We also obtained *K*-band images with IRCAM on the United Kingdom Infrared Telescope (UKIRT), with a total exposure of 2160 s at a scale of 0.″6 pixel^{-1}, as well as three 600 s "snapshot" maps with the VLA[3] A-array configuration at 6 cm.

Our first spectroscopic observations of the jet were carried out at the Cassegrain focus of the Canada-France-Hawaii 3.6 m telescope (CFHT) in 1986, using the Institute for Astronomy (IfA) wide-field grism spectrograph and the Galileo/IfA TI 500 × 500 CCD. A three-slice image slicer served as the input aperture of the spectrograph, and the central slit was aligned along the jet and through the QSO, at position angle 120°. We obtained two 3600 s exposures at a reciprocal dispersion of 4.0 Å pixel^{-1}, and the final reduced spectrum covered the wavelength region from 5097 to 6415 Å.

A second set of spectra, with a total integration of 20,400 s divided among five exposures, was obtained at the University of Hawaii 2.2 m Telescope in 1989, using the IfA faint-object spectrograph and a TI 800 × 800 CCD from the NSF distribution. For these spectra, a 4.″7 wide slit was aligned across the jet, at position angle 30°, and with the slit centered 5″ from the QSO. The CCD output was binned 2 × 2, giving a reciprocal dispersion of 2.8 Å per binned pixel and a wavelength range from 4509 to 5484 Å.

We carried out standard CCD reduction procedures and spectral extraction, using IRAF for the 1989 data and Zodiac (an IfA-developed image reduction and analysis package) for the 1986 data. The calibrated spectra differed slightly in the overlap region, presumably because of the differing regions of the jet sampled by the effective entrance apertures used, and the 1986 spectrum was adjusted by a small scale factor before the spectra were combined.

2.3. *The Nature of the Jet*

At least superficially, the jet bears some resemblance to the well-known jet of 3C 273, and the two QSOs have other similarities, including a strong flat-spectrum nuclear radio source and rapid X-ray variability. The spectral-energy distribution of the OX 169 jet, as derived from our photometric measurements, is compared with that of the 3C 273 jet in Figure 3. The two are not strongly distinguished by the optical and infrared data, but the upper limit for the OX 169 jet at 5 GHz shows that the two spectra are, in fact, substantially different. The radio-optical spectral index for the 3C 273 jet is −0.98, whereas for the OX 169 jet it must be greater than −0.65.

The evidence on the nature of the OX 169 jet that finally persuades us that any similarities to the 3C 273 jet are indeed superficial is the optical spectrum of it presented in Figure 4. The spectrum is clearly stellar in origin. The dashed curve shows the spectrum of the bulge of M31 for comparison: not only are the continuua similar in shape, but several common spectral features are present. The spectrum of the jet is somewhat earlier than that of the M31 bulge (note the weakness of the CN band just shortward of the Ca II H and K lines), and the integrated spectral type near rest wavelength 4000 Å appears to be around F8 or G0.

These results indicate that the term "jet," implying a long narrow structure, is very likely inappropriate for this feature (although, for convenience, we will continue to use it throughout the remainder of this paper). The actual stellar distribution,

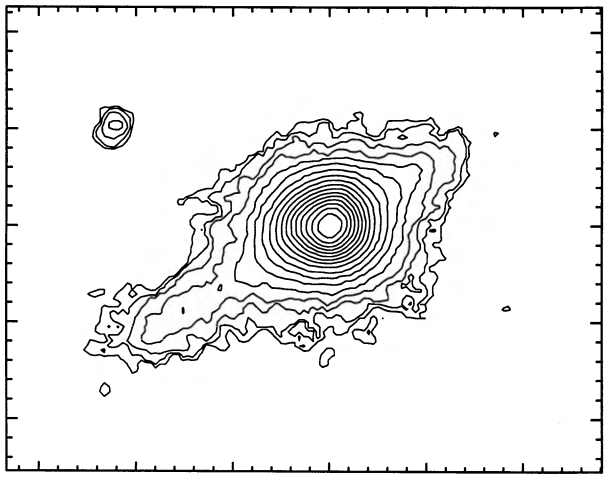

FIG. 2.—Contour plot of an image obtained at the f/35 Cassegrain focus of the University of Hawaii 2.2 m telescope with the Galileo/IfA TI 500 × 500 CCD. The total exposure was 4050 s through a filter passing 5730 to 6230 Å. The outermost contour corresponds approximately to *R* mag 25.6 per square arcsec, and the contour interval is 0.5 mag. The orientation is the same as for Fig. 1, and the tick marks indicate arcsec units.

[3] The National Radio Astronomy Observatory is operated by Associated Universities, Inc., under cooperative agreement with the National Science Foundation.

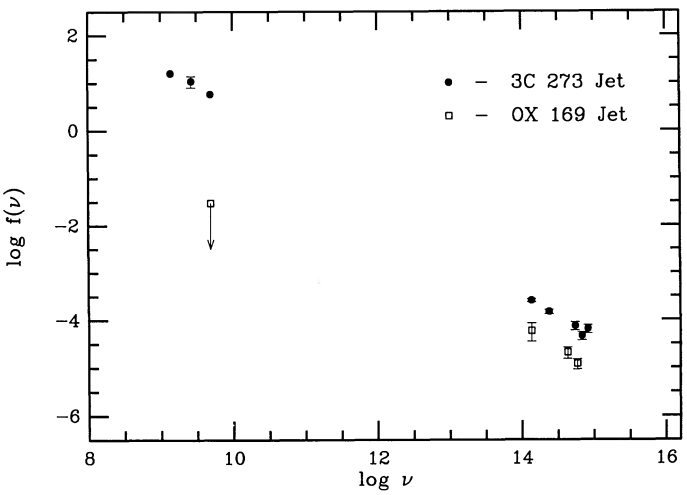

FIG. 3.—Spectral-energy distributions for the jets associated with 3C 273 and OX 169.

comprised as it is of a substantial population of old stars, is much more likely to be a plane, viewed edge-on. It is clear that there is a strong preferential selection for the detection of such an edge-on distribution, but we can point to at least two QSOs for which we may be seeing similar features more nearly face-on: 3C 48 and Mrk 1014. Both of these have one-armed spiral continuum features (Stockton 1990 and references therein), and the one associated with Mrk 1014 is confirmed to have a stellar spectrum (MacKenty & Stockton 1984). Our observations of OX 169 suggest that these two objects may be only the most luminous extreme of a distribution, the fainter examples of which may be virtually undetectable unless they are viewed nearly edge-on.

3. THE BROAD-LINE PROFILES

3.1. *Introduction*

The interpretation of the broad-line profiles in the spectrum of the QSO itself has generated some controvery. When Smith (1980) first pointed out the fact that the broad Balmer lines were double-peaked, he favored an explanation in terms of Balmer self-absorption in a broad-line cloud along the line of sight to the continuum source. This conclusion was based largely on the facts that the broad-line profiles of Hα, Hβ, and Hγ were similar and symmetric, each with an apparent sharp self-reversal near the line center, and that these profiles had not varied sensibly over a 2 yr time span. He pointed out that structure in the broad-line profiles of two other objects, IC 4329A and 3C 390.3, had been attributed instead to a corresponding velocity structure in the broad-line cloud ensemble, but that in these cases the Balmer-line profiles varied from one line to another or with time, respectively.

Another possibility was suggested by Gaskell (1981), who noticed that the blueward peak of the Balmer lines in OX 169 appeared to agree fairly closely in velocity with the forbidden lines. He therefore found it plausible that the character of the Balmer-line profiles should be explained as one of the by no means rare cases of a substantial difference in velocity between the broad and narrow lines (Gaskell 1982), the blue peak, on this interpretation, being due to narrow-line Balmer emission, while the red peak would be the true peak of the broad-line profile.

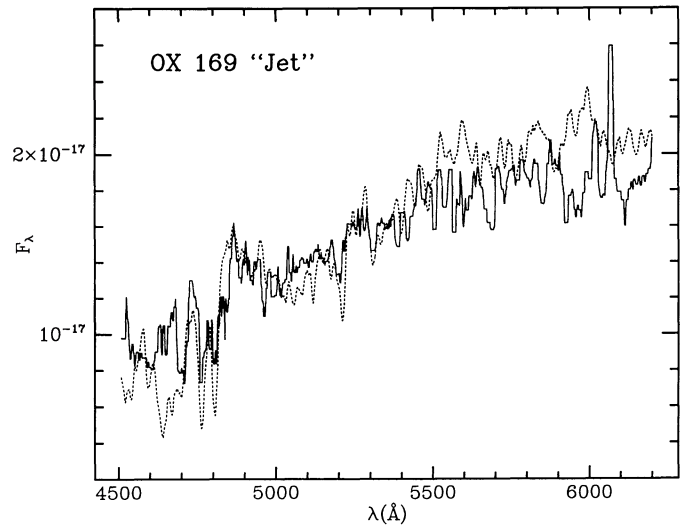

FIG. 4.—Spectrum of the OX 169 jet (*solid line*), compared with the spectrum of the bulge of M31 (*dotted line*) redshifted to $z = 0.21$. The spectrum of the jet is clearly of stellar origin and of somewhat earlier spectral type than the bulge of M31.

3.2. *Observations*

Both Smith's and Gaskell's spectroscopy were obtained at fairly low resolution. We have obtained spectroscopy at higher resolutions and signal-to-noise ratios at two epochs 6 yr apart, using in each case the University of Hawaii 2.2 m telescope faint-object spectrograph. The spectrum of 1983 September 8 had an exposure time of 9000 s on the Galileo/IfA TI 500 × 500 CCD, with a resolution (FWHM of unresolved lines) of 7.3 Å. The more recent spectrum combines data obtained on 1989 September 2 and 3, with a total exposure of 10,200 s on a TI 800 × 800 CCD and a resolution of 5 Å. The spectra have been calibrated to absolute intensity units, though with some uncertainty due to the different slit widths used and to variations in the seeing conditions encountered. In order to have a basis for comparison of spectra taken under different conditions several years apart, we have made the assumption that the intensity of the narrow lines is constant and that the narrow-line region is unresolved. This last assumption is not rigorously correct, since (as Fig. 4 shows) we see very weak extended emission in the jet, but it is certainly close enough to the truth for our purposes.

3.3. *Analysis of the Broad-Line Profiles*

The spectrum of OX 169 for the region around Hβ obtained on 1983 September 8 is shown in Figure 5. What is impressive about the Hβ profile is not only its symmetry, but the sharpness and depth of the apparent central absorption. Because our confidence in the details of this profile is going to be important for our later discussion, we need here to establish the degree to which we can trust them.

The principal potential worry is that the night-sky Na D doublet falls near the center for the Hβ profile. Even though sky-subtraction errors would not generally be a major concern for a 15.5 mag object, we have taken two independent approaches to the sky subtraction. First, we have simply averaged the sky on the two sides of the continuum and subtracted this spectrum from the average over the object continuum. Second, we have used the IRAF "background" task to fit a smooth cubic spline function to the sky background in each

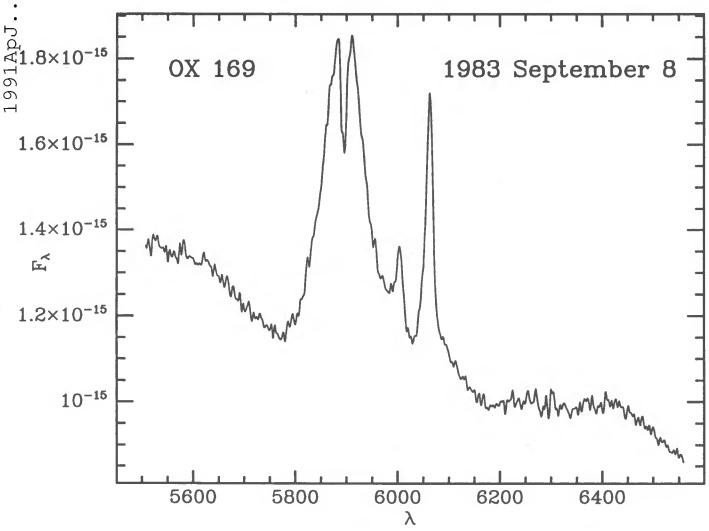

FIG. 5.—Spectrum of OX 169 Hβ region obtained on 1983 September 8

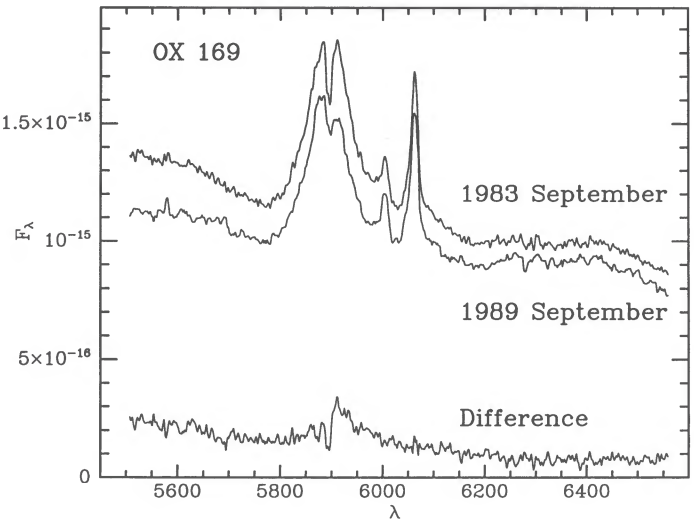

FIG. 7.—Spectra of OX 169 obtained in 1983 and 1989, and their difference spectrum.

row (i.e., perpendicular to the dispersion). Although the latter technique gave smaller residuals in the regions covered by the stronger night-sky lines, the two approaches gave virtually identical Hβ profiles. Figure 6 shows a surface plot of the Hβ region of the original frame (i.e., prior to sky subtraction); it is clear that the noise in the Na D feature is quite small compared with the amplitude of the apparent absorption.

The 1983 September spectrum is shown again in Figure 7, along with a spectrum that combines data obtained on 1989 September 2 and 3 and that has been normalized so that the intensity of the [O III] lines is the same as for the earlier spectrum. Three main differences between the spectra are apparent: (1) the continuum is both weaker and redder in the more recent spectrum, (2) the central "absorption" is less pronounced, and (3) the redward Hβ peak is comparatively weaker. Figure 7 also shows the difference between the two spectra on the same scale. The difference spectrum shows a broad-line profile at the redshift of the redward component of the original Hβ spectrum, on which are superposed a pair of narrow apparent absorption features. Note that there is no indication of a broad-line component at the position of the blueward peak. An attempt to fit a profile to the residual, ignoring the apparent absorption, is shown in Figure 8.

From a purely phenomenological perspective, we take this variation as evidence that there are at least two essentially independent components of the broad-line region. Furthermore, if we now assume that the shape of the profile of the broad line in the difference spectrum is typical of that of the redward component of Hβ in the QSO spectrum, we can attempt a deconvolution of the total Hβ profile. This assumption could be in error if the time scale for continuum variability were short compared to the light-travel time across the broad-line region; however, we are using it only as a starting point.

We first attempt a crude subtraction, simply scaling our fit

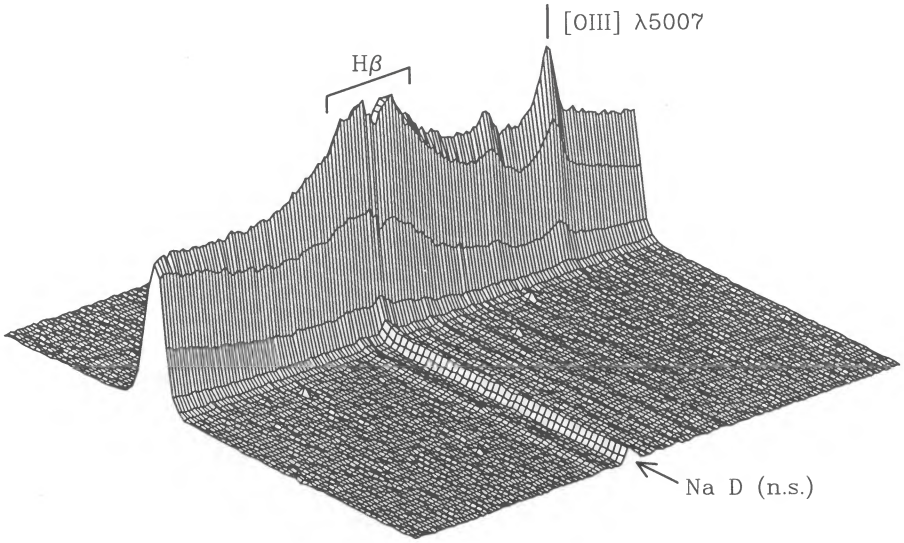

FIG. 6.—Surface plot of 1983 September 8 spectrum prior to sky subtraction

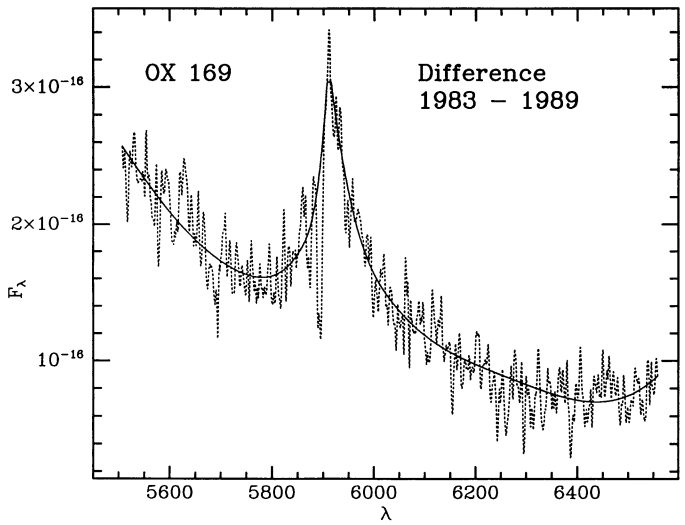

FIG. 8.—Difference between the 1983 and 1989 spectra (*dotted line*); fit to difference spectrum (*solid line*).

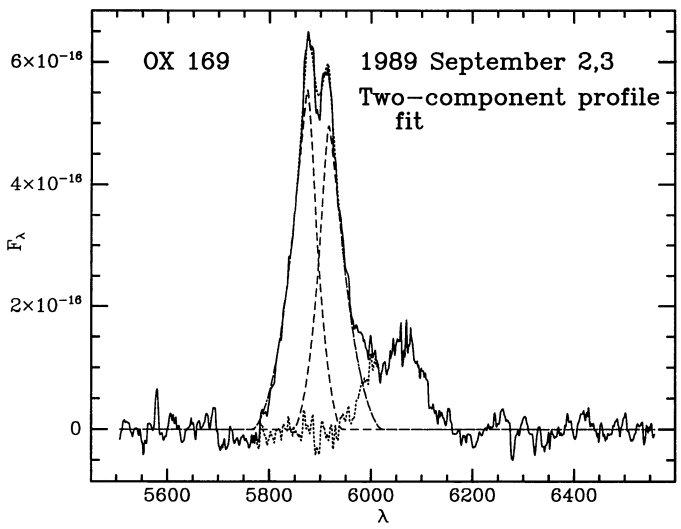

FIG. 10.—1989 Hβ profile (*solid line*), components of fit (*dashed lines*), composite fitted profile (*upper dotted line*), and difference between observed profile and fit (*lower dotted line*).

to the difference profile. Figure 9 shows the original 1989 September spectrum, with the continuum removed and a scaled version of the fit to the difference line profile subtracted. The remaining Hβ profile is clearly also a broad-line profile; in fact, its width is very similar to that of the redward component we have just subtracted. Note also that both of the profiles are asymmetric and have their steepest slopes toward the center of the combined profile. This suggests that we might consider a simple deconvolution of the whole Hβ profile, using components of identical shape (but mirror-imaged), scaled appropriately.

Before we go further, it is worthwhile to consider sources of contamination of the Hβ profile and to remove what we can. We can fairly easily determine a narrow-line profile from the [O III] λ5007 line and subtract it off along with the [O III] λ4959 line, which comes from the same upper level and has one-third the intensity of λ5007. We adopt a typical ratio of the narrow-line component of Hβ to [O III] λ5007 of 0.10. After subtracting off these narrow lines, we are clearly left with some broad-line contamination on the red wing of Hβ. This may include broad components of the [O III] lines as well as Fe II λλ4924, 5018. We have no good way of identifying and removing these components with the necessary accuracy, so we simply ignore the lower portion of the red wing of the Hβ profile in evaluating our fits.

Even with the constraint of mirror symmetry for our fitted components, the solution is by no means unique. One reasonable fit to the 1989 profile is shown in Figure 10, and a similar fit to the 1983 profile is shown in Figure 11. The component profiles used for these fits have been constrained to be the same for both epochs, except that the scaling and centering have been allowed to vary to give the best match to the total profile. The intensity of the blue component of the Hβ profile decreased by 7% from 1983 to 1989, and that of the red component decreased by 26% over the same time. In addition, it

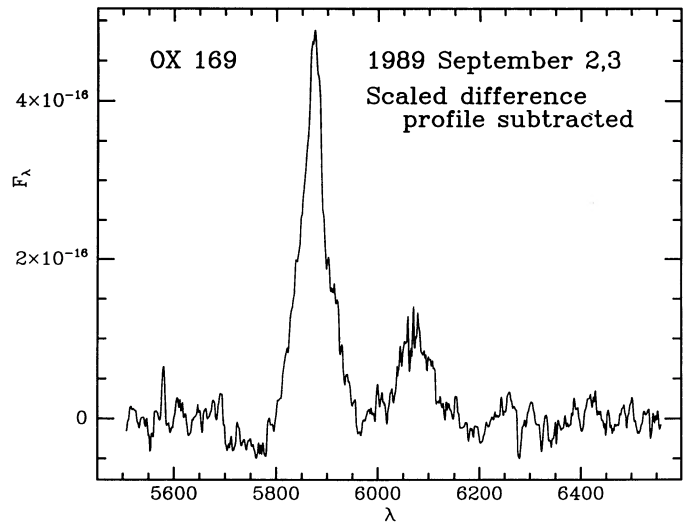

FIG. 9.—Spectrum of OX 169 Hβ region obtained in 1989, with scaled fit to the 1983–1989 difference profile subtracted.

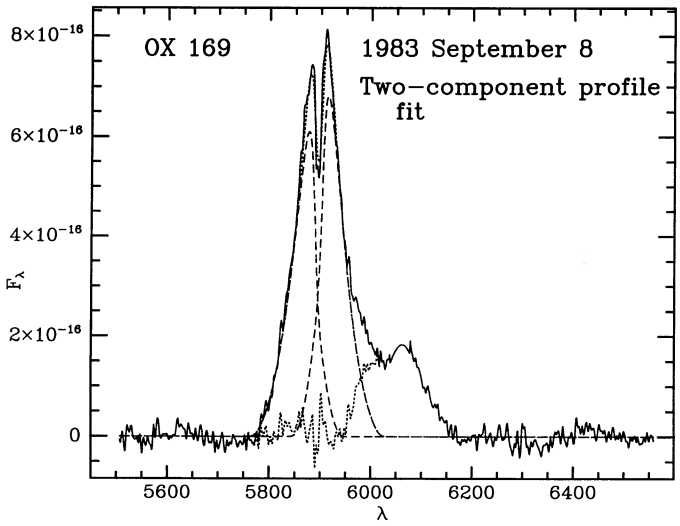

FIG. 11.—Same as Fig. 10, for 1983 Hβ profile

was necessary to decrease the separation of the two components by about 2 Å in order to obtain an adequate fit to the 1989 profile, but this result could simply be an artifact of our assumption that the profiles have not varied, apart from scaling factors (see § 4.2 for further discussion).

3.4. *Broad-Line Region Models*

3.4.1. *Balmer Self-Absorption*

Smith's (1980) proposal was that the double-peaked broad-line profiles in OX 169 were due to Balmer absorption in a broad-line cloud along the line of sight. The main attractions of this suggestion are that it allows the broad-line region in OX 169 to be similar to those of the great majority of other active nuclei and that it explains the difference in steepness between the sides of the absorption and emission profiles in a natural way. On the other hand, the absorption cloud would have to almost completely cover the continuum source, and it is not clear that a cloud of this sort is consistent with other inferences concerning broad-line clouds in QSOs. The most telling objection to this suggestion, however, is that it cannot easily explain the change in the relative strength of the red and blue sides of the profiles between 1983 and 1989.

3.4.2. *Accretion Disk*

The Balmer line profiles in OX 169 bear a striking resemblance to emission-line profiles seen in cataclysmic variables (see, e.g., Stover 1981). In these systems, the emission lines arise in a disk of material accreting from a red giant onto a degenerate companion; such a disk has a tidally determined maximum radius, and the absence of low-velocity gas leads to a pronounced dip at the line center. Quite apart from this particular instance, it has been extremely tempting to try to interpret the broad-line profiles of AGN in terms of disk models (Osterbrock 1978; van Groningen 1983): the standard model for AGN involves an accretion disk in any case, and gas with the requisite velocities to produce the wings of the broad line profiles is almost certainly present.

While the basic idea is attractive, it has proven to be extraordinarily difficult to work out the details (see, e.g., Mathews 1982; Dumont & Collin-Souffrin 1990). We restrict ourselves here to the question of whether a Keplerian disk with some reasonable emission function can fit our line profiles, using the formalism developed by Chen & Halpern (1989). Briefly, the emissivity of the disk is assumed to both rise and fall as a power-law function of radius, with an additional exponential cutoff at large radii. The shape of the observed line profile is defined by the parameters required to give the emissivity of the disk (the power-law index q and two radii, ξ_1 and ξ_2; see Chen & Halpern, eq. [2]) and the inclination of the disk to the line of sight. A calculated line profile is compared with the 1989 Hβ profile in Figure 12. The fit to the wings of the profile is astonishingly good, and the general character of the center of the profile is reproduced. The asymmetry in the line wings is due to gravitational redshift, and the blue peak is always higher than the red peak for these models because of Doppler boosting.

It is this last effect that prevents us from achieving an acceptable fit to the 1983 data with a model of this type, as Figure 13 shows. The same model fit as was used for Figure 12 has been scaled to fit the wings of the profile; as before the fit to the wings is very good, but no such model can fit a profile having a red peak higher than the blue peak. A model that incorporates broad-line emisson from a jet as well as a disk has been suggested in other contexts (van Groningen 1983). However, such

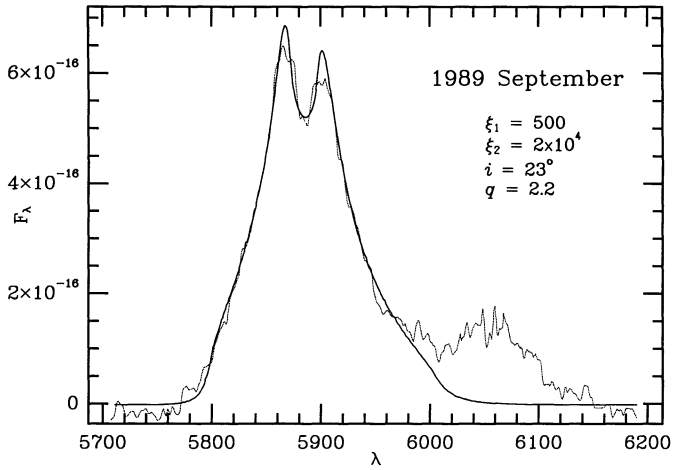

FIG. 12.—Disk emission model (*solid line*) fitted to 1989 Hβ profile (*dotted line*).

a solution seems unlikely for OX 169, because the variable emission from the jet would have to have a redshift that closely matches that of the red peak from the accretion disk.

One might consider invoking azimuthal terms in the assumed emissivity for the disk, but at such a point, the disk models begin to lose much of their attractive conceptual simplicity, and the physical basis for the observed profile variations is not clear. Also not addressed by these strictly kinematic models are the differences among Balmer line profiles at the same epoch. As Figure 14 shows, OX 169 follows the usual rule that the Balmer lines get broader as one goes up the series. This trend demonstrates that the Balmer decrement is correlated with position within the broad-line region and is a clear indication that optical depth effects are important in determining the observed line profiles. In order to properly evaluate whether disk models for the broad-line region are in reasonable agreement with observed profiles, one would really want models that self-consistently incorporate radiative processes. Dumont & Collin-Souffrin (1989; see also references therein) have calculated some such profiles (in the nonrelativistic approximation) and find that Hβ indeed does have more extended wings than Hα; however, their models also appear to

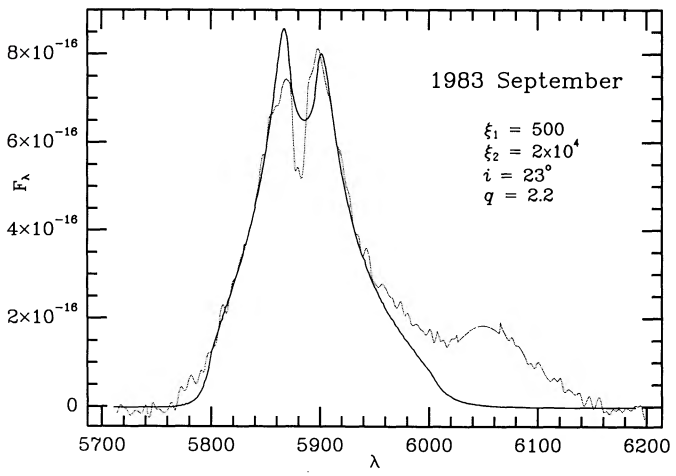

FIG. 13.—Same as Fig. 12, for 1983 Hβ profile

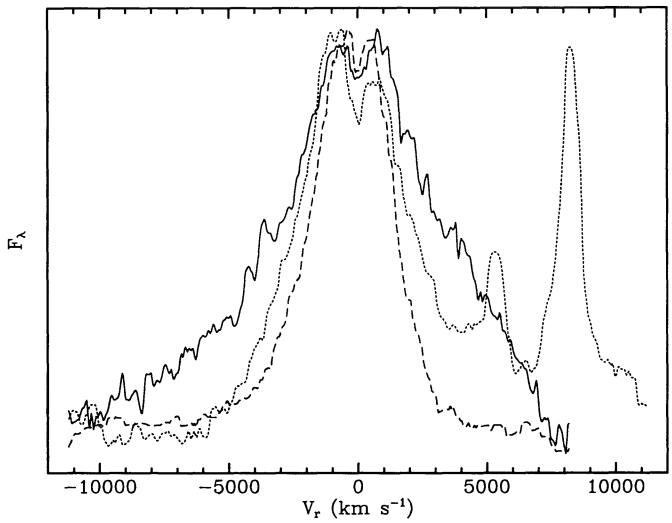

FIG. 14.—Profiles of Hα (*dashed line*), Hβ (*dotted line*), and Hγ (*solid line*) obtained in 1989 September, normalized to the same peak value and plotted in velocity units in the reference frame of OX 169.

show much stronger differences between the two lines in the cores of the profiles than we observe in OX 169.

3.4.3. *Supermassive Binary*

The original proposal by Gaskell (1981) that the two peaks in the Balmer line profiles in OX 169 were simply due to a large velocity difference between the narrow-line and broad-line redshifts is no longer tenable, since both components of the profile are broad. However, Gaskell (1983) later pointed out that in such discrepancies between broad and narrow-line redshifts (which are not particularly uncommon), it is virtually certain that it is the broad lines that are displaced from the systemic velocity, and he suggested that the most likely explanation for these displacements was that these nuclei hosted two supermassive objects. In most cases, only one of these would be strongly active, resulting in a single, displaced broad-line region; but occasionally one might end up with two independent broad-line regions. The idea that supermassive binaries might form during galaxy mergers had earlier been suggested to explain cases of precession of radio jets and was given theoretical credence by Begelman, Blandford, & Rees (1980), who showed that after an initial rapid evolution such binaries can achieve a long-lived ($>10^8$ yr) quasi-stable state.

We have argued that the most direct interpretation of the broad Balmer-line profiles in OX 169 is that two independent broad-line regions are present. The acceptance of two distinct broad-line regions need not *necessarily* imply a supermassive binary, in that one can imagine configurations of broad-line clouds, either alone, or in conjunction with selective obscuration, that might result in the observed profile while requiring only a single continuum source: in particular, certain kinds of bipolar outflow seem possible (Foltz, Wilkes, & Peterson 1983; Zheng, Binette, & Sulentic 1990). Nevertheless, the binary hypothesis has certain attractions, particularly in its ability to account in a natural way for the observed symmetry between redshifts and blueshifts of the broad lines relative to the narrow lines. For OX 169, the peaks of the components into which we resolve the Hβ profile are at velocities of −490 and +1400 km s^{-1} in the frame defined by the redshift of the narrow lines. If the narrow-line redshift were identical to the center-of-mass velocity of the presumed binary, the velocity asymmetry would give a mass ratio of 2.9. The objection has been made (Chen, Halpern, & Filippenko 1989) that a binary broad-line region is not simply the sum of two independent broad-line regions: in particular, that the low-velocity clouds that contribute most strongly to the core of the profile will not be bound to the individual supermassive objects but will rather orbit the center of mass of the two. But this objection holds only if (1) the separation of the peaks of the two broad-line profiles is comparable to the width of each, and (2) the motions of the broad-line clouds are dominated by gravitational forces. Furthermore, if, as seems possible, the process of formation of the supermassive binary results in the loss of the less strongly bound, lower velocity clouds altogether, then, while it would be true that the broad-line profile from the binary would not be the linear superposition of the two original independent broad-line regions, the profile would still have a pronounced double peak.

4. DISCUSSION

4.1. *The Jet*

4.1.1. *Evidence in Favor of a Tidal Origin*

We have shown that the "jet" of OX 169 is composed of stars and is most likely an asymmetric planar feature, like those associated with 3C 48 and Mrk 1014, seen edge-on. If this is the case, it probably would not have been detected if its orientation had been more nearly face-on. Thus, the three examples of these curious "one-armed spirals" out of ∼40 luminous, low-redshift QSOs with at least moderately deep images may be only the most tractable cases of a fairly widespread phenomenon.

We are not aware of any reasonable interpretation of such global asymmetries as these involving *old* stars other than that they are tidal features. There are no evident close companions to OX 169 (a galaxy 38″ to the west has the same redshift [Stockton 1978], but it shows no sign of interaction and is probably too distant to be considered a potential culprit); presumably either the companion is too close to the QSO to be distinguished, or (perhaps more likely) it has already merged.

How confident can we be in such a merger scenario? The key point is that, for both OX 169 and Mrk 1014, we can identify spectral features characteristic of F- to G-type stars, i.e., indicative of a stellar population far older than any plausible dynamical time scale for these asymmetries. This means that the stars cannot have been formed in situ, by, say, jet-induced star formation. Whatever process is responsible, it has to be able to modify the orbits of already formed stars in a collective manner, and it is difficult to conceive of any nongravitational force doing so.

4.1.2. *Could the Stars Be Young?*

A possible escape from the line of reasoning just given would be to appeal to some process that allows star formation with a grossly truncated mass function, so that virtually no high-mass stars are formed; such mass functions have been proposed for star formation from cooling flows (Sarazin & O'Connell 1983). Then the late-type stellar spectrum we observe could still arise in a young stellar population, consistent with the dynamical time scale of the feature. We can estimate the star formation rate required on this assumption from the probable dynamical lifetime of the structure (we take 2×10^8 yr) and the mass implied by its luminosity and a simple mass function consistent with our photometry. We adopt the usual power-law parameterization of the mass function (i.e., $dN/dm \sim m^{-(1+x)}$) for the

lower main sequence and find the index that best fits the photometry. Stellar spectral-energy distributions for F5, G0, G5, K0, K5, M0, M5, and M8 dwarfs were approximated by fitting smooth curves to flux densities derived from representative U, B, V, I, and K photometry. Masses and relative V luminosities for these types were taken from Allen (1973), and crude synthetic spectra were computed from the individual normalized stellar spectrum for different mass function indices. The best fit to the photometry was with an index $x = 2.5$. For this quite steep mass function, we calculate a total mass of 1.5×10^{11} $M_\odot$. This figure is likely to be still quite conservative, since the mass may very well be dominated by even lower mass "stars," which make negligible contribution to the observed luminosity. (In our simple model, the luminosity at the K band is dominated by M5 stars; M8 stars, which comprise 65% of the mass, contribute only 17% of the total K luminosity.) However, if we take this mass at face value and note that, for any sort of continuous star formation process, the observed morphology would have been smeared out over a time scale of about 2×10^8 yr, we obtain a minimum average star formation rate of 750 $M_\odot$ yr^{-1}.

While *cooling rates* approaching this figure have been claimed in some rich clusters (Crawford et al. 1989, and references therein), inferred *star formation* rates are typically a few orders of magnitude lower. The required efficiency of star formation, the total mass involved, and the apparent focusing of the process on a region well outside the galaxy all would make any cooling-flow interpretation of OX 169 look forced, particularly since there are no examples of similar types of star formation associated with strong nearby cooling flows.

In summary, even if a steep, truncated mass function is invoked in order to allow the stars in the jet to be younger than the dynamical lifetime of the feature which being consistent with the photometry, the total mass approaches that of a giant galaxy and the star formation rate required is unreasonably large. If, on the other hand, the jet is actually a tidal feature, it can comprise an evolved stellar population with giants dominating the K-band luminosity, leading to flatter mass function and a much lower total mass.

4.2. *The Broad-Line Region*

4.2.1. *Evaluation of Different Models*

We have looked at different possible explanations for the double-peaked Balmer-line profiles of OX 169. Which of these is most consistent with the observations? Here we give considerable weight to the time variations in the profile. The fact that the difference between our 1983 and 1989 Hβ profiles gives a residual dominated by a broad-line component at the redshift of the redward peak argues strongly in favor of a model involving two more or less independent broad-line regions. Standard broad-line profiles with Balmer self-absorption cannot explain the time variation we see, and a rotating disk would require contrived time-varying azimuthal asymmetries.

Some perspective on the plausibility of various models can be gained by considering other active galaxies with broad, double-peaked Balmer-line profiles, such as 3CR 390.3 (Osterbrock, Koski, & Phillips 1976; Perez et al. 1988), OQ 280 (Osterbrock & Cohen 1979; Gaskell 1983), Arp 102B (Stauffer, Schild, & Keel 1983; Halpern & Oke 1986; Halpern & Filippenko 1988), and Akn 120 (Peterson et al. 1983, 1985; Alloin, Boisson, & Pelat 1988). Taken singly, these objects have elicited a variety of interpretations: accretion disks (Perez et al. 1988; Chen & Halpern 1989), bipolar outflow (Foltz, Wilkes, & Peterson 1983; Zheng, Binette, & Sulentic 1990), and selective obscuration (Osterbrock & Cohen 1979). However, as Sulentic et al. (1990) have emphasized, the fact that, taken as a group, these show no bias in whether the blue or red peak is stronger or in direction of displacement from the systemic redshift makes the standard accretion disk model untenable as a general explanation for the double-peak phenomenon. The same can be said for selective obscuration models, unless one is willing to countenance inflow for some objects and outflow for others (Gaskell 1983). Bipolar outflow models can be given a sufficient number of free parameters so that a large range of profile shapes can be fitted (Zheng, Binette, & Sulentic 1990), but they do require that the emission properties of the broad-line clouds be essentially isotropic in order to avoid a preferential bias in the line shifts by differences between the approaching and receding flows. Supermassive binaries avoid such biases but may run into trouble from the lack of observed changes in the radial velocities of the peaks for objects with large peak displacements and small inferred masses (Halpern & Filippenko 1988).

Thus, to the extent that we insist on a single physical mechanism for the range of double-peaked broad-line phenomena present in active galaxies, these objects reinforce our conclusion that models involving a single, contiguous broad-line region have great difficulty in explaining the observations. We believe that a supermassive binary, each component having its own broad-line region, is consistent with the observed profiles; but other kinds of models involving separate, distinct broad-line regions may also be possible. Note, however, that supermassive binaries have the virtue of accounting for other phenomena: as we have mentioned earlier, Begelman et al. (1980) found them attractive as an explanation for precessing radio jets, and Gaskell (1983) felt that they were the most natural explanation for the frequent displacement of the broad lines from the systemic velocity.

4.2.2. *Detection of Orbital Motion?*

Aside from resolution of the individual nuclei, the most direct test of the supermassive binary hypothesis would be the observation of radial velocity variations consistent with orbital motion. As we mentioned in § 3.3, in order to achieve the best fit of the Hβ profile with the same component profiles used to fit the 1983 data, we had not only to scale the components but also to decrease their separation by about 2 Å. Is it at all plausible that we might here be seeing changes in radial velocity due to orbital motion? The orbital period is given by $\tau = 2962[R_{\rm pc}^3/M_9]^{1/2}$ yr, where $R_{\rm pc}$ is the separation between the two nuclei in parsecs, M_9 is their combined mass in units of 10^9 $M_\odot$, and we have assumed that dynamical friction will have circularized the orbits. If V_r is the difference in radial velocity between the two components (in the frame local to the QSO), then

$$\frac{dV_r}{dt} = -4.40 \frac{M_9}{R_{\rm pc}^2} \sin i \sin \theta \text{ km s}^{-1} \text{ yr}^{-1} ,$$

where i is the inclination of the orbit to the plane of the sky and θ is the longitude of the binary axis with respect to the intersection of the orbit with the plane of the sky. If we take the 102 km s^{-1} (QSO frame) apparent change in relative radial velocity over 6 yr seriously and assume that we are viewing the plane of the orbit edge-on ($\sin i = 1$), Figure 15 shows that for a wide range of θ, plausible values of $R_{\rm pc}$ and M_9 are consistent with the amplitude and rate of change of the relative radial velocity.

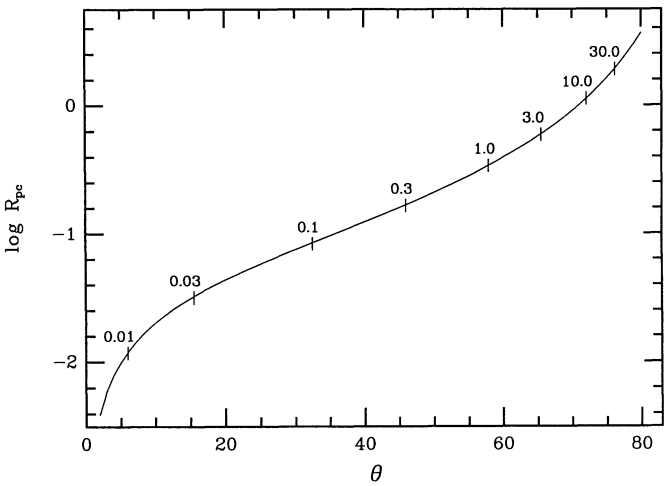

FIG. 15.—Locus of separations R_{pc} as a function of orbital longitude θ for a supermassive binary with an observed mean differential radial velocity (in the QSO frame) of 1890 km s^{-1} and a variation in this value of 102 km s^{-1} over a 6 yr period, assuming that the line of sight lies in the plane of the orbit. The numbers on the curve give the total mass of the binary in units of $10^9\ M_\odot$.

While the suggestion that there has been a radial velocity variation between the broad-line components in OX 169 is tantalizing, we ourselves put little credence in the present evidence: the difference in velocity is too strongly dependent on the assumption of constancy of the component profile shapes. At this stage our result can only serve to motivate continued observations.

4.3. *A Unified View of OX 169*

It can hardly have escaped the reader's attention that our interpretations of the two very different observational phenomena we have been discussing have in some sense converged. We have argued that when we see global asymmetries on the scale of the jet of OX 169 and have evidence that they comprise an old stellar population, there can be little doubt that gravitational interaction is responsible. While we have not similarly emphasized the origin of the putative supermassive binary, certainly one of the most plausible mechanisms is through the merger of two galaxies, each harboring a single supermassive object. In a merger, the two nuclei coalesce rapidly under the influence of dynamical friction and the characteristic time scale for the formation of a long-lived supermassive binary (Begelman et al. 1980) can be short compared with the lifetime of large-scale signatures of the interaction, such as tails. Thus, if the broad-line profiles are indeed indicative of a supermassive binary, this binary *may* have resulted from the same interaction responsible for the jet.

There are at least some points of self-consistency in this position. The fact that the jet is both narrow and straight indicates that the disk from which it originated is aligned with our line of sight and that the plane of the mutual orbit of the two interacting galaxies is not too different, providing some justification for our assumption that sin $i = 1$ when we were calculating whether we might reasonably be able to detect the effect of orbital motion in a few years. And the fact that we detect a fairly strong tidal *tail* indicates that the interacting galaxies were of comparable mass (Toomre & Toomre 1972), which makes it at least plausible that the two black holes might be similar, as observed.

Evidence that strong interactions and mergers may be important in triggering nuclear activity in QSOs has been discussed for nearly a decade now, and the roots of the idea go back to early papers by Toomre & Toomre (1972) and Gunn (1979) (see Stockton 1990 and Heckman 1990 for recent reviews). It is important to reemphasize that interactions have several possible signatures (bridges, tails, distorted close companions, enhanced star formation, etc.); whether any one or more of these is produced in any given case depends on such factors as the relative masses of the interacting galaxies, the presence or absence of a stellar disk, the gas content and distribution within the galaxies, the relative orientations and rotation vectors of the galaxies, and their orientation with respect to our line of sight. We are still somewhat unsure of the significance of the examples of apparent interactions involving QSOs that have been cited, because of the lack of a suitable control sample; we can only say, first, that it is impressive that we can detect *any* fairly unequivocal interaction signatures at the redshifts involved, leading us to suspect that there must be many more that we do not detect; and second, that even to account for the numbers of apparent interactions we *do* see, it appears that the frequency of such interactions among the galaxy population in general would have to rise quite sharply in going from the present to the epoch of $z \sim 0.3$ if there were no relationship between interactions and activity.

Direct evidence for supermassive binaries in active nuclei has been scarcer and more controversial, even though there are fairly strong theoretical and circumstantial observational reasons for believing that they exist and play a significant role. The essential missing piece of evidence is unambiguous detection of orbital motion. If a significant number of binaries exist with masses greater than $10^8\ M_\odot$ and periods less than 200 yr, careful observations should be capable of uncovering them within the next decade.

We thank Bill Mathews and Sylvain Veilleux for helpful discussions and Carrie Yoshimura for suggesting improvements to the text. Comments by the referee, Eric P. Smith, have also helped us improve the presentation. CCD development at the Institute for Astronomy has been partially supported by NSF grant AST-8615621, and the TI 800 × 800 CCDs were provided under NSF grant AST-8514575. This work was supported in part by NSF grant AST-8715330.

REFERENCES

Allen, C. W. 1973, Astrophysical Quantities (London: Athlone)
Alloin, D., Boisson, C., & Pelat, D. 1988, A&A, 200, 17
Begelman, M. C., Blandford, R. D., & Rees, M. J. 1980, Nature, 287, 307
Chen, K., & Halpern, J. P. 1989, ApJ, 344, 115
Chen, K., Halpern, J. P., & Filippenko, A. V. 1989, ApJ, 339, 742
Crawford, C. S., Arnaud, K. A., Fabian, A. C., & Johnstone, R. M. 1989, MNRAS, 236, 277
Dumont, A. M., & Collin-Souffrin, S. 1990, A&A, 229, 313
Feigelson, E. D., Isobe, T., & Kembhavi, A. 1984, AJ, 89, 1464
Foltz, C. B., Wilkes, B. J., & Peterson, B. M. 1983, AJ, 88, 1702
Gaskell, C. M. 1981, ApJ, 251, 8
———. 1982, ApJ, 263, 79
———. 1983, in Quasars and Gravitational Lenses, Proc. 24th Liège Ap. Colloquium (Liège: Université de Liège, Institut d'Astrophysique), 473
Gehren T., Fried, J., Wehinger, P. A., & Wyckoff, S. 1984, ApJ, 278, 11
Gower, A. C., & Hutchings, J. B. 1984, AJ, 89, 1658
Gunn, J. E. 1979, in Active Galactic Nuclei, ed. C. Hazard & S. Mitton (Cambridge: Cambridge Univ. Press), 213
Halpern, J. P., & Filippenko, A. V. 1988, Nature, 331, 46
Halpern, J. P., & Oke, J. B. 1986, ApJ, 201, 753

Heckman, T. M. 1990, in IAU Colloquium 124, Paired and Interacting Galaxies, ed. J. W. Sulentic, W. C. Keel, & C. M. Telesco (NASA CP-3098), in press
Heckman, T. M., Smith, E. P., Baum, S. A., van Breugel, W. J. M., Miley, G. K., Illingworth, G. D., Bothun, G. D., & Balick, B. 1986, ApJ, 311, 526
Hutchings, J. B., Crampton, D., & Campbell, B. 1984a, ApJ, 280, 41
Hutchings, J. B., Crampton, D., Campbell, B., Duncan, D., & Glendenning, B. 1984b, ApJS, 55, 319
MacKenty, J. W., & Stockton, A. 1984, ApJ, 283, 64
Mathews, W. G. 1982, ApJ, 258, 425
Osterbrock, D. E. 1978, Proc. Nat. Acad. Sci., 75, 540
Osterbrock, D. E., & Cohen, R. 1979, MNRAS, 187, 61P
Osterbrock, D. E., Koski, A. T., & Phillips, M. M. 1976, ApJ, 206, 898
Perez, E., Penston, M. V., Tadhunter, C., Mediavilla, E., & Moles, M. 1988, MNRAS, 230, 353
Peterson, B. M., Foltz, C. B., Miller, H. R., Wagner, R. M., Crenshaw, D. M., Meyers, K. A., & Byard, P. L. 1983, AJ, 88, 926
Peterson, B. M., Meyers, K. A., Capriotti, E. R., Foltz, C. B., Wilkes, B. J., & Miller, H. R. 1985, ApJ, 292, 164
Sarazin, C. L., & O'Connell, R. W. 1983, ApJ, 268, 552
Smith, E. P., Heckman, T. M., Bothun, G. D., Romanishin, W., & Balick, B. 1986, ApJ, 306, 64
Smith, H. E. 1980, ApJ, 241, L137
Stauffer, J., Schild, R., & Keel, W. 1983, ApJ, 270, 465
Stockton, A. 1978, ApJ, 223, 747
———. 1990, in Dynamics and Interactions of Galaxies, ed. R. Wielen (Heidelberg: Springer-Verlag), in press
Stockton, A., & MacKenty, J. W. 1987, ApJ, 316, 584
Stover, R. J. 1981, ApJ, 248, 684
Sulentic, J. W., Calvani, M., Marziani, P., & Zheng, W. 1990, ApJ, 355, L15
Thuan, T. X., & Gunn, J. E. 1976, PASP, 88, 543
Toomre, A., & Toomre, J. 1972, ApJ, 178, 623
van Groningen, E. 1983, A&A, 126, 363
Zamorani, G., Giommi, P., Maccacaro, T., & Tananbaum, H. 1984, ApJ, 278, 28
Zheng, W., Binette, L., & Sulentic, J. W. 1990, ApJ, 365, 115